

Advanced Modelling and Optimization of Infrared Oven in Injection Stretch Blow-moulding for Energy Saving

Ziqi Yang*, Wasif Naeem*, Gary Menary**, Jing Deng*,
Kang Li*

* *School of Electronics, Electrical Engineering and Computer Science,
Queen's University Belfast, Belfast, BT9 5AH, UK (e-mail:
zyang06@qub.ac.uk, k.li@qub.ac.uk, j.deng@qub.ac.uk,
w.naeem@ee.qub.ac.uk).*

** *School of Mechanical & Aerospace Engineering, Queen's University
Belfast, Belfast, BT9 5AH, UK (e-mail: g.menary@qub.ac.uk)*

Abstract:

In the production process of polyethylene terephthalate (PET) bottles, the initial temperature of preforms plays a central role on the final thickness, intensity and other structural properties of the bottles. Also, the difference between inside and outside temperature profiles could make a significant impact on the final product quality. The preforms are preheated by infrared heating oven system which is often an open loop system and relies heavily on trial and error approach to adjust the lamp power settings. In this paper, a radial basis function (RBF) neural network model, optimized by a two-stage selection (TSS) algorithm combined with particle swarm optimization (PSO), is developed to model the nonlinear relations between the lamp power settings and the output temperature profile of PET bottles. Then an improved PSO method for lamp setting adjustment using the above model is presented. Simulation results based on experimental data confirm the effectiveness of the modelling and optimization method.

Keywords: Infrared Heating Oven, Nonlinear Modelling, Optimization

1. INTRODUCTION

Over the last few decades, the use of plastics has experienced significant growth due to its numerous merits such as lightweight with high strength, high temperature and chemical resistance, easy to mould with relatively low cost. One of its applications is in the carbonated soft drink and mineral water industries where injection stretch blow-moulding (ISBM) processes are employed to make numerous thin-walled polyethylene terephthalate (PET) bottles. In the ISBM process, the polymer preforms are first loaded and conveyed in an infrared heating oven. The heated preforms are then stretched and blown to produce to the final shape in a metal blow mould. Due to the fast production rate, the ability to mould complex parts and some other distinctive features, the ISBM process has become one of the most popular plastics processing methods in the polymer industry.

In the PET bottle production process, the initial temperature of preforms plays a central role during the ISBM process. The final thickness and other structural properties of PET bottles are highly dependent on the temperature profile of preforms (Bordival et al. [2009]). Further, the difference between inside and outside temperature profiles

could have a significant impact on the processing behavior and properties of the final product. Therefore, the preform temperature is one of the most important parameters in the PET bottles production (ISBM) process.

However, most current infrared heating ovens used in ISBM do not have on-board sensors to measure the internal and external temperatures of preforms on line, and it is also very expensive and difficult to install infrared temperature sensors to measure the preform temperatures in the existing machines. Luo et al. [2012] used an infrared camera's sensor to build a finite element model. However only external temperature could be obtained and model accuracy is low. Further, feedback controller is rarely used in the infrared heating oven system, and almost all facilities are open loop and lamp parameters are adjusted by trial and error, which leads to a significant waste of time and energy in addition to the additional operation cost (Menary et al. [2010]).

To obtain an accurate preform temperature profile while reducing the energy waste, it is necessary to apply advanced optimization methods to the infrared heating oven system to obtain the appropriate lamp settings. As it is difficult to measure the temperature in real-time and adjust lamp settings on-line automatically, a mathematical model is necessary for optimization and testing. Hence, a radial basis function (RBF) neural network model optimized by two-stage selection (TSS) algorithm combined

* This work was partially supported by EPSRC under grants EP/G059489/1 and EP/F021070/1, and Technology Commission of Shanghai Municipality under Grant 11ZR1413100. Ziqi Yang would like to thank the China Scholarship Council for the financial support.

with particle swarm optimization (PSO) is developed for an infrared heating oven system. Then, an improved PSO method for lamp settings adjustment is designed to obtain desired temperature profiles.

This paper is organized as follows. The experimental equipment set-up and temperature data acquisition for system modelling are introduced first in Sections 2 and 3 respectively. Section 4 presents the system model and simulation results. An improved PSO method for lamp settings adjustment and experimental results are given in Section 5. Finally, Section 6 concludes the paper and suggests the future work.

2. EXPERIMENTAL SET-UP

2.1 The Configuration of Infrared Heating Oven

The infrared heating oven and stretch blow-moulding machine used in this research was manufactured by VITALII & SON and is available in the polymer processing research center (PPRC) at Queens University Belfast. The preforms used in this experiment are 18.5g PET bottles with a diameter of 30mm at the mouth (see Fig. 1).

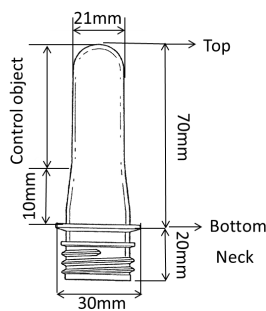


Fig. 1. Structure of 18.5g PET preform

The layout of the infrared heating oven is shown in Fig. 2 and Fig. 3. Two guards (between points B and C, H and I) are installed in front of the infrared heating oven for safety. There are a number of preform bases on the machine belt which can be seen in Fig. 3. The preform is placed on the bases between points I and B, and then conveyed anticlockwise into the oven. When the preform arrives at point D, the base starts to spin anticlockwise in order to heat the preform evenly around the circumference. There are eight infrared lamp tubes from bottom to top (No. 1 to No. 8) on both sides of the machine (between point D - E and F - G).

As the preform has a height of 90mm, five lamp tubes (No.1 - No.5) are deemed sufficient to heat the given preforms. However, for a different-sized preform, it may be required to use the remaining lamp tubes. Once the preform arrives at point I, it is removed from the base and placed on the THERMOscan to determine its temperature profile. The THERMOscan is an equipment used to measure the internal and external surface temperature of the preform (more details see www.bmt-ni.com).

The machine transport velocity is an important parameter, which could be adjusted from 13.18 mm/s to 18.67 mm/s. At the maximum transport velocity, the entire heating process for a single preform is 129 seconds. In this paper,

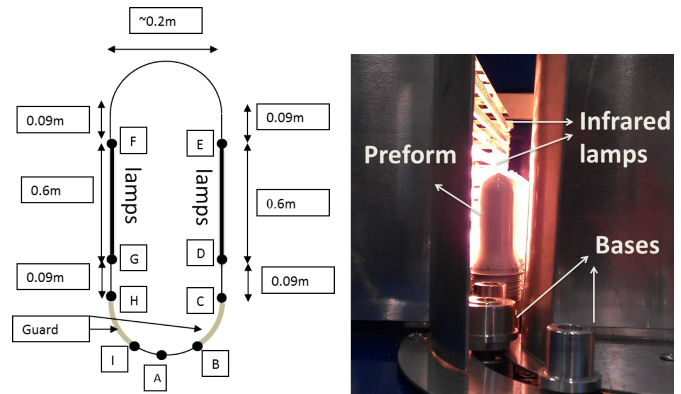


Fig. 2. The structure of in- Fig. 3. Diagram of lamps and preform infrared heating oven

the transport velocity is set constant at the maximum value for simplicity, and therefore is not included in the modelling process.

2.2 Temperature profiles measurement

As there are no on-board temperature sensors to detect the preform temperature profile within the experimental oven, an indirect measurement method is designed.

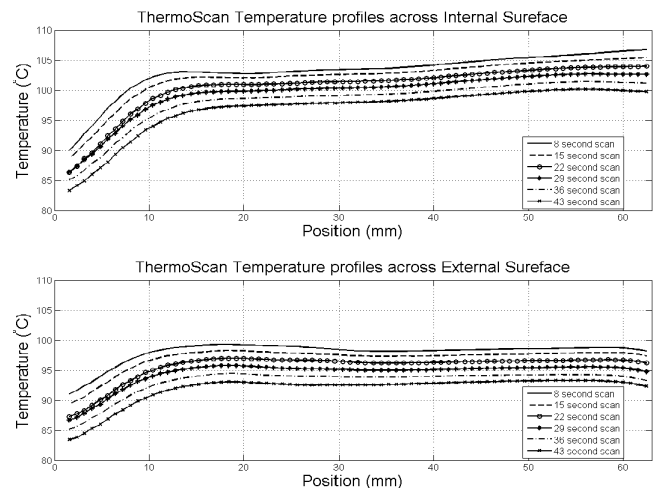


Fig. 4. THERMOscan average temperature profile across internal and external surface

When the preform is heated, it is manually removed from the oven and placed on the THERMOscan. The internal and external preform temperatures are measured at 84 points from bottom to top, thus constituting the internal and external temperature profile of the complete preform. It should be noted that there is a small delay between the completion of the preform heating process and the temperature profile measurement by the THERMOscan. In order to compensate for the temperature loss during that time, 6 scan results are automatically carried out to calculate the correct temperature profile with an error margin. Then 14 data points from bottom to top are obtained to present the complete heated temperature profile of the preform. Fig. 4 presents the internal and external temperature profiles at different time after the preforms have left oven. For each point along the surface, the scan logs are interpolated to gain a knowledge of

the change in temperature. The data obtained from the THERMOscan was processed to obtain the internal and external temperature profiles of the preform after leaving the oven.

3. EXPERIMENTS OF PREFORMS HEATING USING INFRARED OVEN

In order to build a preform temperature profile model related to the oven lamp settings, a series of experiments need to be carried out to generate the required data. For this purpose, the maximum and minimum infrared lamp settings should be calculated first. This is because overheating the preform at high temperature results in crystallization making the preform too stiff to process. On the other hand, too low settings will result in too low of temperature to enable the preform to be blown.

A heuristic method was used to test the range of infrared lamps power settings. Firstly, the power of all the lamps was set to 45% of the maximum value. After the heating process, it was observed that the top section of the preform was crystallised meaning that the settings were too high for the top lamps. Given this observation, the settings for all heating lamps were reduced. However, the crystallization of the top section still occurred but with smaller crystallised area. Then, only lamps 4 and 5 were further reduced as the crystallised area was confined to the top section of the preform. This process was repeated until the maximum setting value for each lamp was found.

To determine the minimum lamp power required values, both internal and external temperatures of preform should be higher than the lowest value which is approximate 90°C. To achieve this goal, tests based on trial and error were used again. The resulting maximum and minimum power settings for each infrared lamp are shown in Table 1.

Table 1: Maximum and minimum settings of each infrared lamp

	Lamp 1	Lamp 2	Lamp 3	Lamp 4	Lamp 5
Max	40%	40%	40%	35%	35%
Min	22%	22%	22%	22%	22%

For data acquisition, 25 combinations of lamp settings were randomly obtained within the constraints as in Table 1. In order to reduce experimental error, each combination was executed twice. The average of two temperature profiles is then taken as the final result. From Fig. 1, since the control object is the temperature from the top of the preform to 10mm from bottom, temperature value from 12 points in each test were used to build the modelling database. A total number of 300 data points for internal and external temperature samples were obtained. In the next section, a model of the infrared heating oven system based on these experimental data will be built. Simulation results will also be shown demonstrating the accuracy from the obtained model.

4. MODELLING OF INFRARED HEATING OVEN SYSTEM

In this paper, a RBF neural network model identified using a heuristic optimization method, namely PSO method

and a TSS selection algorithm is presented, which models the internal and external preform temperature profiles in correlation to the lamp power settings.

As a non-linear identification method, the RBF network is recognised as a universal approximation model and has been used for fault diagnosis, prediction, classification, modelling and control (Chen and Billings [1992]). Compared to the multilayer perception neural network, RBF neural network is easier to train because it has a simple topological structure. In the construction of the RBF network model, the output layer weights are relatively easier to obtain by the least-squares method. However, it is difficult to achieve the non-linear basis function parameters. Traditional methods such as exhaustive search or gradient methods could be implemented, but they are often computationally expensive and do not achieve the global best.

In this paper, a heuristic approach, namely the PSO (Eberhart and Kennedy [1995]) is introduced. The employment of PSO in RBF network model can be used to achieve both global and local best solutions by optimizing the non-linear and linear parameters (Deng et al. [2011]). However, because a number of particles and iterations are needed in the optimization process, it can also be computationally expensive. In comparison, the TSS algorithm (Li et al. [2005] and Deng et al. [2012a]) has the ability to reduce computation cost by selecting fewer parameter to be optimized step by step. So the combination of PSO and TSS could achieve both the global best optimal solution and desirable computational efficiency. A brief review of RBF, PSO and TSS are presented below.

4.1 Radial Basis function network model

A general RBF neural model can be expressed as

$$y(t) = \sum_{k=1}^n \theta_k \varphi_k(\mathbf{x}(t); \mathbf{c}_k; \boldsymbol{\Sigma}_k) + \varepsilon(t) \quad (1)$$

where $y(t)$ denotes the system output at sample time t , $\mathbf{x}(t) \in \mathbb{R}^p$ represents the input vector, $\varphi_k(\mathbf{x}(t); \mathbf{c}_k; \boldsymbol{\Sigma}_k)$ is the RBF activation function, $\mathbf{c}_i = [c_{i1}, c_{i2}, \dots, c_{ip}]^T$ is the centre vector, and $\boldsymbol{\Sigma}_i$ represents the associated norm matrix including the range of the width of RBF centres σ_i . Finally, θ_k denotes the output layer weight for each RBF node, and $\varepsilon(t)$ represents the network error at sample time t . By using a set of N data samples $\{\mathbf{x}(t), y(t)\}_{t=1}^N$ for model training, (1) can then be re-written in a matrix form as

$$\mathbf{y} = \boldsymbol{\Phi} \boldsymbol{\theta} + \mathbf{e} \quad (2)$$

If the regression matrix $\boldsymbol{\Phi}$ is of full column rank, the least-squares estimate of the regression coefficients in (2) is given by

$$\hat{\boldsymbol{\theta}} = (\boldsymbol{\Phi}^T \boldsymbol{\Phi})^{-1} \boldsymbol{\Phi}^T \mathbf{y} \quad (3)$$

where $\boldsymbol{\Phi}^T \boldsymbol{\Phi}$ is called the information matrix. The associated minimal cost function is

$$J_n(\hat{\boldsymbol{\theta}}_n) = \mathbf{y}^T (\mathbf{I} - \boldsymbol{\Phi}_n) (\boldsymbol{\Phi}_n^T \boldsymbol{\Phi}_n)^{-1} \boldsymbol{\Phi}_n^T \mathbf{y} \quad (4)$$

4.2 Particle Swarm Optimization

PSO is an optimization algorithm which optimizes a problem by iteratively searching for best solution from ran-

domly candidate solutions. In this work, PSO has been utilised for non-linear parameters optimization in the hidden layer of RBF neural network model.

Suppose \mathbf{x}_i represents the i^{th} particle in the swarm, \mathbf{v}_i denotes its velocity, \mathbf{p}_i is its best position to date, while \mathbf{p}_g represents the best position from the entire swarm. $\mathbf{v}_{(i+1)}$ and $\mathbf{x}_{(i+1)}$ are updated as:

$$\mathbf{v}_{(i+1)} = w_0\mathbf{v}_i + c_1r_1(\mathbf{p}_i - \mathbf{x}_i) + c_2r_2(\mathbf{p}_g - \mathbf{x}_i) \quad (5)$$

$$\mathbf{x}_{(i+1)} = \mathbf{x}_i + \mathbf{v}_i \quad (6)$$

where w_0 is the inertia weight used to scale the previous velocity term, c_1 and c_2 are acceleration coefficients, and r_1 and r_2 are two uniform random numbers generated between 0 and 1. The acceleration coefficients c_1 and c_2 can be fixed or varied during the iterative procedure.

In order to ensure that each updated particle is still inside the search space, it is also necessary to define a value range, and check both the position and velocity for each particle at the end of an iteration.

4.3 The two-stage selection algorithm

The two-stage selection algorithm includes a forward model construction stage and a backward model refinement stage.

First stage - forward selection. At this stage, the nonlinear parameters \mathbf{c}_i and θ_k of RBF model are optimized by the selection of the local best and global best particles by the PSO, and added to the model at each step. The initial particle value at each stage is chosen randomly and the significance of each centre is measured by its contribution to the cost function. This selection process continues until some satisfactory modelling criteria are obtained or until the maximum number of centres are chosen. Then the algorithm moves to the second stage.

Second stage - backward refinement. The model from forward selection is not optimal because of the correlations between selected terms. At this stage, the significance of each previously selected centre is reviewed, and all insignificant ones are replaced. Clearly, the last selected centre in the forward construction has always been maximally optimized for the whole network. The backward refinement can be divided into two main steps: (a) a selected centre is moved to the last position in such a way that it was regarded as the last selected one; (b) an alternative center is found by optimization, and its local and global best values are substituted for the selected centre based on the rest of re-ordered centres. If the moved one is less significant than the new generated centre it will be replaced, leading to the required improvement in reducing training error and generalisation capability. Moreover, PSO is used to find the best centre at each step. More details about the algorithm was shown in [Deng et al., 2011] and [Deng et al., 2012b].

4.4 Modelling and testing results

The internal and external infrared heating oven models are built respectively in this section. There were 300 data points each for internal and external preform temperatures. 276 points from each were used for RBF model training, and the other 24 were reserved for model validation.

For each data point, five lamp settings and the position on the preform are set as the six model inputs, while the temperature value is the model output. All the data were normalized and the order was randomized to guarantee training effect. The TSS algorithm integrated with PSO was then applied on the training data.

Table 2: Modelling performances of temperature profile

Model	Model size	Training error	Test error
External	6	0.7482	0.4909
Internal	6	0.6707	0.4088

Table 3: Optimized parameters in the RBF model for the external preform temperature prediction

PRM	Optimized values
θ_1	1.2310
θ_2	-5.9951
θ_3	2.6533
θ_4	2.8325
θ_5	-3.9581
θ_6	4.4984
\mathbf{c}_1	[1.2000, 1.2000, 1.2000, 0.9539, 0.4705, 0.4068]
σ_1	[2.0000, 2.0000, 2.0000, 2.0000, 0.8881, 2.0000]
\mathbf{c}_2	[0.2394, 0.0677, 0.4213, 0.3979, 0.0987, 0.5242]
σ_2	[1.8697, 2.0000, 2.0000, 2.0000, 2.0000, 2.0000]
\mathbf{c}_3	[0.1102, 0.2991, 0.9274, 0.5468, 0.4837, 0.7252]
σ_3	[1.9718, 1.9718, 1.9718, 1.9718, 1.9718, 1.9718]
\mathbf{c}_4	[1.2000, 1.2000, 0.5150, 0.4718, 0.9092, 1.1906]
σ_4	[2.0000, 2.0000, 2.0000, 2.0000, 2.0000, 2.0000]
\mathbf{c}_5	[0.9182, 0.8574, 0.3000, 0.4092, 0.6561, 0.7977]
σ_5	[2.0000, 2.0000, 2.0000, 2.0000, 2.0000, 2.0000]
\mathbf{c}_6	[0.6772, 0.3950, 0.1191, 0.2781, 0.1029, 0.4580]
σ_6	[1.9859, 1.4774, 1.9859, 1.9859, 1.9859, 1.9859]

Table 4: Optimized parameters of RBF model for the internal preform temperature prediction

PRM	Optimized values
θ_1	21.2947
θ_2	-1.7368
θ_3	1.7558
θ_4	3.7339
θ_5	-21.3050
θ_6	-1.8344
\mathbf{c}_1	[1.2000, 1.2000, 1.2000, 0.6483, 0.3564, 1.2000]
σ_1	[2.0000, 2.0000, 2.0000, 2.0000, 2.0000, 2.0000]
\mathbf{c}_2	[0.6513, 0.1989, 0.8793, 0.4102, 0.3654, 0.8572]
σ_2	[1.8045, 2.0000, 2.0000, 1.9897, 2.0000, 2.0000]
\mathbf{c}_3	[0.5201, 0.5837, 1.2000, 0.9947, 0.4745, 1.2000]
σ_3	[2.0000, 2.0000, 2.0000, 2.0000, 0.4955, 2.0000]
\mathbf{c}_4	[1.2000, 0.7885, 0.5865, 0.2094, 0.0000, 0.5234]
σ_4	[2.0000, 2.0000, 2.0000, 2.0000, 2.0000, 2.0000]
\mathbf{c}_5	[1.2000, 1.1517, 1.0647, 0.5347, 0.3009, 1.0865]
σ_5	[2.0000, 2.0000, 2.0000, 2.0000, 2.0000, 2.0000]
\mathbf{c}_6	[0.3838, 0.0092, 0.4687, 0.6632, 0.1194, 0.2788]
σ_6	[1.7325, 2.0000, 2.0000, 2.0000, 2.0000, 2.0000]

In the modelling, the range of the width of RBF centres was set as $\sigma_i \in [0.1, 2.0]$. The particle number was 50 and update iteration number was 50. Table 2 shows the validation results where the root mean square error is employed for evaluator training and testing performance. The training and test performances of both external and

internal temperatures profiles are also shown in Fig. 5 - Fig. 8. The associated RBF model parameters are given in Table 3 and Table 4.

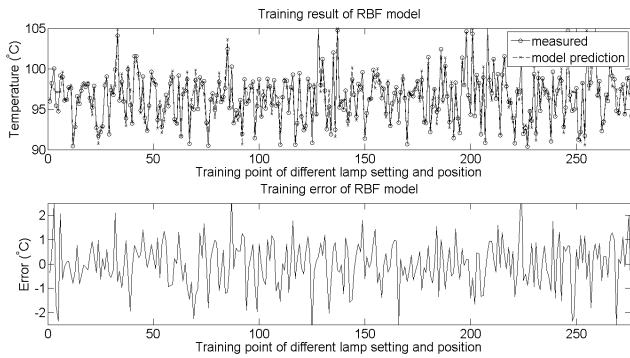


Fig. 5. The preform external temperature model training performance by TSS+PSO

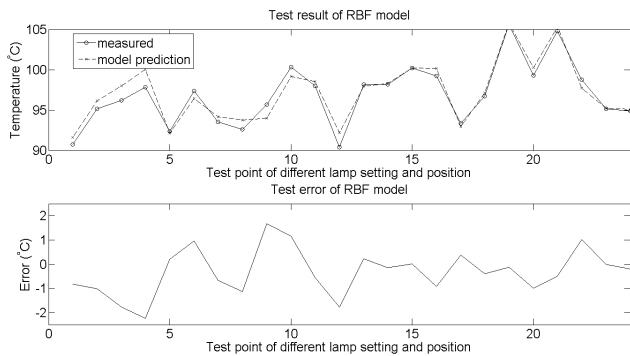


Fig. 6. The preform external temperature model test performance by TSS+PSO

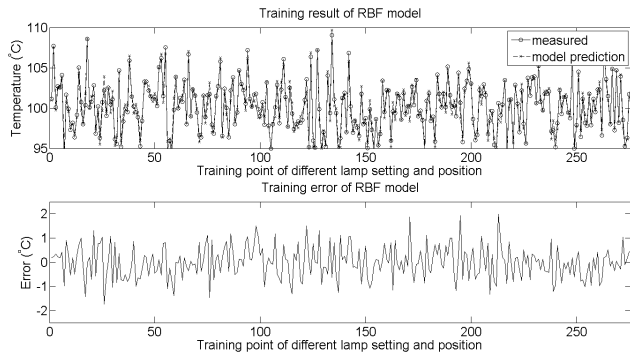


Fig. 7. The preform internal temperature model training performance by TSS+PSO

5. PSO OPTIMIZATION OF INFRARED HEATING OVEN LAMP SETTINGS

The resulting internal and external preform temperature models were employed to find the optimal settings of the infrared heating oven lamps. Because of the static nature of the temperature profile models, feedback control cannot be applied. Also there appears to be strong coupling between the lamps. For these reasons, PSO as a meta-heuristic optimization method has been utilised to obtain appropriate lamp settings for the desired preform temperature profiles.

As shown in Equation (5), the velocity update law of each particle is based on the momentum term $w_0 \mathbf{v}_i$, the

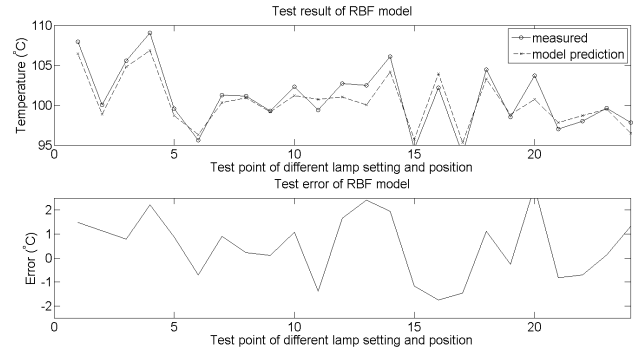


Fig. 8. The preform internal temperature model test performance by TSS+PSO

cognitive part $c_1 r_1 (\mathbf{p}_i - \mathbf{x}_i)$ and the social part $c_2 r_2 (\mathbf{p}_g - \mathbf{x}_i)$. In order to increase the searching efficiency and accuracy, the parameters are set as below:

$$\begin{aligned} w_0 &= (0.8 - 0.5)l/l_m ax + 0.5 \\ c_1 &= (1 - 3)l/l_m ax + 3 \\ c_2 &= (3 - 1)l/l_m ax + 1 \end{aligned} \quad (7)$$

The particle number is 50 and the update iteration number is 300. The optimized lamp settings for different desired temperature profiles are given in Table 5. The optimized performance of simulation results compared with desired temperature profiles are shown in Fig. 9 - Fig. 12.

For the external temperature, the error between the desired and simulated temperature is quite small for the uniform temperature setting of 101 °C (Fig. 9). The error is no more than 0.3 °C for a linear variation in the desired external temperature setting from 97 - 101 °C (Fig. 10). And 0.5 °C error could be seen at top and bottom section when the internal temperature setting is uniform 106 °C (Fig. 11). While, Fig. 12 shows good performance for a linear variation in the desired internal temperature settings. From these results, it is observed that all the error of different experiments are in a small range. And in the ISBM process, 1 °C error is acceptable for preform temperature profile. So the results of this improved PSO method are accurate enough for real ISBM process.

Table 5: Optimized lamp settings for different desired temperature

Temp. (°C)	Lamp settings	Ref.
101	[37.7 38.1 29.4 26.5 31.5]	Fig. 9
97 - 101	[29.4 26.8 26.4 28.0 31.1]	Fig. 10
106	[38.4 29.1 38.8 31.6 27.3]	Fig. 11
103 - 111	[25.8 33.9 37.4 30.9 34.0]	Fig. 12

6. CONCLUSION AND FUTURE WORK

Preform temperature plays a central role in the ISBM process to produce plastic bottles with desired properties. During the heating process, the preform is heated by several infrared lamp tubes in the infrared heating oven. Due to the lack of closed-loop control, large variations can be observed on the preform temperature. As the temperature cannot be measured on line, in order to obtain optimal lamp settings, a mathematical model is needed. In this work, based on the experimental data, a RBF neural

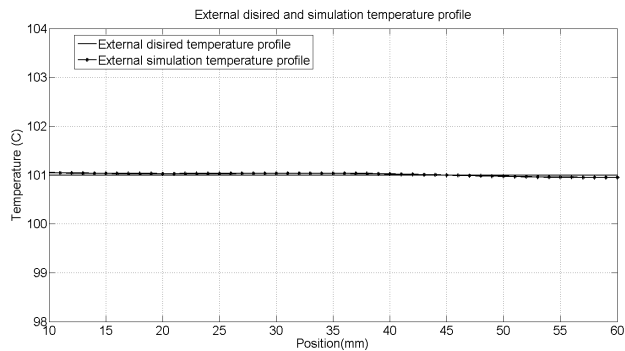


Fig. 9. Comparison of external desired (101°C) and simulation temperature profile

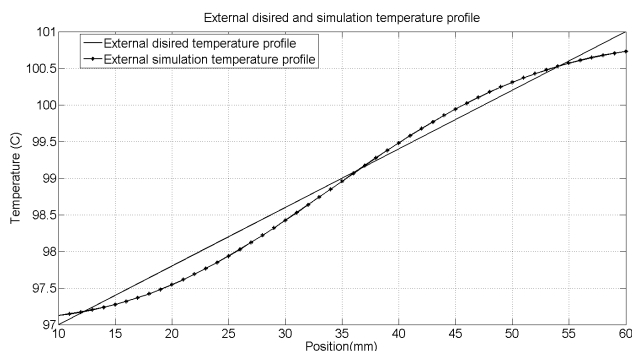


Fig. 10. Comparison of external desired ($97^{\circ}\text{C} - 101^{\circ}\text{C}$) and simulation temperature profile

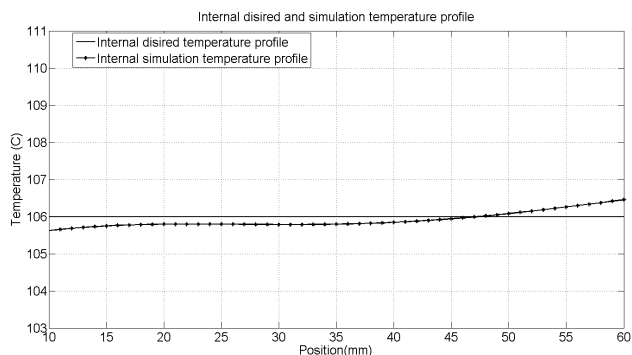


Fig. 11. Comparison of internal desired (106°C) and simulation temperature profile

network model optimized by two-stage selection algorithm combined with PSO has been developed and the simulation results have confirmed its feasibility and accuracy. An improved PSO method has been implemented to optimize lamp settings and simulation results show its efficacy. Future work will improve the accuracy of the system model and optimized parameters. The optimization method can be further improved for adjusting the lamp settings to achieve better and more desirable internal and external temperature profiles simultaneously.

ACKNOWLEDGEMENTS

The authors would like to thank reviewers for their constructive comments.

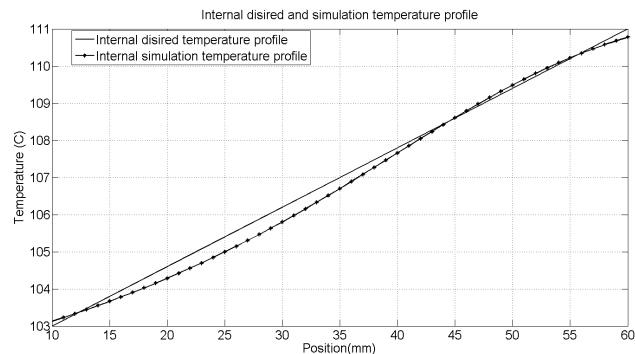


Fig. 12. Comparison of internal desired ($103^{\circ}\text{C} - 111^{\circ}\text{C}$) and simulation temperature profile

REFERENCES

- M. Bordival, F.M. Schmidt, Y. Le Maout, and V. Velay. Optimization of preform temperature distribution for the stretch-blow molding of pet bottles: Infrared heating and blowing modeling. *Polymer Engineering & Science*, 49(4):783793, Apr 2009. ISSN 00323888, 15482634. doi: 10.1002/pen.21296.
- S Chen and SA Billings. Neural networks for nonlinear dynamic system modelling and identification. *International Journal of Control*, 56(2):319–346, 1992.
- J. Deng, K. Li, G. W. Irwin, and M. Fei. Two-stage RBF network construction based on particle swarm optimization. *Transactions of the Institute of Measurement and Control*, 35(1):2533, Jun 2011. ISSN 0142-3312, 1477-0369. doi: 10.1177/0142331211403795.
- Jing Deng, Kang Li, and George W Irwin. Locally regularised two-stage learning algorithm for RBF network centre selection. *International Journal of Systems Science*, 43(6):1157–1170, 2012a.
- Jing Deng, Ziqi Yang, Kang Li, Gary Menary, and Eileen Harkin-Jones. Heuristically optimized RBF neural model for the control of section weights in stretch blow moulding. In *Control (CONTROL), 2012 UKACC International Conference on*, pages 24–29. IEEE, 2012b.
- Russell Eberhart and James Kennedy. A new optimizer using particle swarm theory. In *Micro Machine and Human Science, 1995. MHS'95., Proceedings of the Sixth International Symposium on*, pages 39–43. IEEE, 1995.
- Kang Li, J-X Peng, and George W Irwin. A fast nonlinear model identification method. *Automatic Control, IEEE Transactions on*, 50(8):1211–1216, 2005.
- Yun Mei Luo, Luc Chevalier, Francoise Utheza, et al. Modelling the heat during the injection stretch blowing moulding: Infrared heating and blowing modelling. In *Proceedings of the ASME 2012 11th Biennial Conference On Engineering Systems Design And Analysis*, 2012.
- G.H. Menary, C.W. Tan, C.G. Armstrong, Y. Salomeia, M. Picard, N. Billon, and E.M.A. Harkin-Jones. Validating injection stretch-blow molding simulation through free blow trials. *Polymer Engineering & Science*, 50(5):10471057, May 2010. ISSN 00323888. doi: 10.1002/pen.21555.